INTERNATIONAL JOURNAL OF COMPUTERS COMMUNICATIONS & CONTROL
*Special issue on fuzzy logic dedicated to the centenary of the birth of Lotfi A. Zadeh (1921-2017)*
Online ISSN 1841-9844, ISSN-L 1841-9836, Volume: 16, Issue: 1, Month: February, Year: 2021
Article Number: 4076, https://doi.org/10.15837/ijccc.2021.1.4076

CCC Publications

# Data-Driven Model-Free Sliding Mode and Fuzzy Control with Experimental Validation

R.-E. Precup, R.-C. Roman, E.-L. Hedrea, E. M. Petriu, C.-A. Bojan-Dragos

**Radu-Emil Precup*, Raul-Cristian Roman, Elena-Lorena Hedrea, Claudia-Adina Bojan-Dragos**
Politehnica University of Timisoara
Department of Automation and Applied Informatics
Bd. V. Parvan 2, 300223 Timisoara, Romania
*Corresponding author: radu.precup@aut.upt.ro
E-mail:raul.roman@aut.upt.ro, lorena.hedrea@aut.upt.ro, claudia.dragos@aut.upt.ro

**Emil M. Petriu**
University of Ottawa
School of Electrical Engineering and Computer Science
800 King Edward, Ottawa, ON, K1N 6N5 Canada
petriu@uottawa.ca

**Abstract**

The paper presents the combination of the model-free control technique with two popular nonlinear control techniques, sliding mode control and fuzzy control. Two data-driven model-free sliding mode control structures and one data-driven model-free fuzzy control structure are given. The data-driven model-free sliding mode control structures are built upon a model-free intelligent Proportional-Integral (iPI) control system structure, where an augmented control signal is inserted in the iPI control law to deal with the error dynamics in terms of sliding mode control. The data-driven model-free fuzzy control structure is developed by fuzzifying the PI component of the continuous-time iPI control law. The design approaches of the data-driven model-free control algorithms are offered. The data-driven model-free control algorithms are validated as controllers by real-time experiments conducted on 3D crane system laboratory equipment.

**Keywords:** data-driven model-free fuzzy control; data-driven model-free sliding mode control; model-free control; 3D crane systems.

## 1 Introduction

Data-driven control is an alternative to model-based control, which is based on model-free controller tuning, where little information on process models is used, and practically considering that no parametric process model is involved. Few iterations or even a single one are usually used in model-free controller tuning. The most successful data-driven model-free control techniques in authors' opinion are: Iterative Feedback Tuning (IFT) [28], [61], [35], Model-Free Adaptive Control (MFAC) [29], [84], Simultaneous Perturbation Stochastic Approximation [73], [85], Correlation-based Tuning [39], [69], Frequency Domain Tuning [38], [12], and adaptive online IFT [43]. These techniques carry out the iterative experiment-based update of controller parameters; however, non-iterative techniques are also popular as Model-Free Control (MFC) [19], [20] expressed as intelligent Proportional-Integral (iPI) control, intelligent Proportional-Derivative (iPD) control and intelligent Proportional-Integral-Derivative (iPID) control, Virtual Reference Feedback Tuning (VRFT) [8], [22], Active Disturbance Rejection Control (ADRC) [25], [64], data-driven predictive control [36], [42], unfalsified control [68], [32], and Data-Driven Inversion Based Control [46], [24]. A review on data-driven control is conducted in [30], and a different view is pointed out in [76] and outlined in [55], stating that here is no need to make the a priori assumption of persistency of excitation on the system input; instead, equivalent conditions are studied on the given data under which different analysis and control problems can be solved, revealing situations in which a controller can be tuned from data even though unique system identification is impossible.

Fuzzy control, as a relatively easily understandable nonlinear control technique and important application of fuzzy sets and systems due to Lotfi A. Zadeh, is transparent versus other similar techniques including those specific to artificial intelligence as, for example, neural network ones, because it can incorporate designer's knowledge and experience. In addition, the sensitivity with respect to modifications of controller and process parameters can be discussed by the appropriate development of sensitivity models [53], [60], [54], [51]. However, as pointed out in [55] and [15], the heuristic approach to design fuzzy controllers is compensated by the systematic design of fuzzy controllers [52], [50], [27], [45]. Model-based fuzzy control and optimal tuning represent two viable directions to the systematic design of fuzzy controllers, requiring the stability guarantee of fuzzy control systems. A discussion on the fresh directions in the stability analysis and stable design of fuzzy control systems is carried out in [55], and some representative results in this regard are reported in[81], [83], [71]. Classical and recent applications of fuzzy control are exemplified in [23], [3], [33], [47], [41], [5], [7], [59].

The advantages of fuzzy control and data-driven model-free control are exploited by the development of different combinations of both algorithms. These combinations include $H_\infty$ fuzzy control [82], fault tolerant fuzzy control [72], parameterized data-driven fuzzy control [37], data-driven interpretable fuzzy control [34], MFC merged with Proportional-Derivative Takagi-Sugeno fuzzy control [63], [67], MFAC merged with Proportional-Derivative Takagi-Sugeno fuzzy control [62], [66], ADRC mixed with Proportional-Derivative Takagi-Sugeno fuzzy control[65] and also tuned by VRFT [18], fuzzy logic-based adaptive ADRC [75], and data-driven arithmetic fuzzy control using the distending function [14].

The effects of data-driven model-free control are also leveraged with those of another popular nonlinear control technique, namely sliding mode control, resulting in mixed data-driven and sliding mode control techniques, briefly pointed out as follows. Sliding mode control is combined with iPI control in [56] and applied to servo systems, next to reverse osmosis desalination plants [77], also formulated as iPD control in [79] and applied to quadrotor systems. A second version of sliding mode control combined with iPI control is suggested in [57] and applied along with that given in [56] to twin rotor aerodynamic systems. Sliding mode control mixed with MFAC is proposed in [80] and applied to robotic exoskeletons. Model-free sliding mode control based on linear regression estimation and optimization is discussed in [16] and applied in [17] to blood glucose control. Sliding mode control is designed by adaptive dynamic programming in [18]. A comparison of several model-free control algorithms in a quadrotor system application is performed in [70]. The combination of discrete-time sliding mode control and MFAC is treated in [9].

This paper offers two contributions with respect to the literature in the field. First, it applies the data-driven model-free sliding mode controllers built upon continuous-time iPI control in the first version in [56], [77] and [57] and the second version in [57] to different challenging nonlinear processes, i.e. three-degree-of-freedom (3D) crane systems. Second, a novel data-driven model-free fuzzy controller is developed by fuzzifying the Proportional-Integral (PI) component of the continuous-time iPI control law. The fuzzy component of the data-driven model-free fuzzy controller, expressed in Takagi-Sugeno form, ensures the bump-less interpolator between three separately designed continuous-time iPI controllers by placing them in the rule consequents. The correct comparison of all controllers is done in terms of the optimal tuning of their free parameters using an appropriately defined optimization problem solved by a metaheuristic Grey Wolf Optimizer (GWO) algorithm, which makes use of the process model in the evaluation of the objective function.

The paper is organized as follows: the iPI controller and the data-driven model-free sliding mode controllers based on it are briefly presented in the next Section. The proposed data-driven model-free fuzzy controller is developed in Section 3. The real-time experimental results focused on the position control of 3D crane system laboratory equipment are offered in Section 4 and the conclusions are highlighted in Section 5.

## 2 Intelligent Proportional-Integral controller and data-driven model-free sliding mode controllers

The continuous-time first-order local process model involved in the design of the iPI controller is [19], [20], [21]

$$\dot{y}(t) = F(t) + \alpha\, u(t), \tag{1}$$

where $F(t)$ is a function that includes the effects of unmodeled dynamics and disturbances, which is estimated using information from the control signal $u(t)$ and the controlled output $y(t)$, and $\alpha > 0$ is a design parameter, chosen by the user such that to ensure the same order of magnitude for $\dot{y}(t)$ and $\alpha\, u(t)$. Defining the tracking error $e(t)$ as

$$e(t) = y(t) - r(t), \tag{2}$$

where $r(t)$ is the reference trajectory (or the set-point trajectory), the control law of the iPI controller is

$$u(t) = \frac{1}{\alpha}(-\hat{F}(t) + \dot{r}(t) - K_P e(t) - K_I \int_0^t e(\tau) d\tau), \tag{3}$$

also expressed as

$$\begin{aligned} u(t) &= \frac{1}{\alpha}(-\hat{F}(t) + \dot{r}(t) - u_{PI}(t)), \\ u_{PI}(t) &= K_P e(t) + K_I \textstyle\int_0^t e(\tau) d\tau, \end{aligned} \tag{4}$$

to point out the PI controller component included, with the output $u_{PI}(t)$ and the transfer function $C(s)$

$$C(s) = K_P + \frac{K_I}{s}, \tag{5}$$

where $K_P$ is the proportional gain of the PI controller, $K_I$ is the integral gain of the PI controller, and $\hat{F}(t)$ is the estimate of $F(t)$ expressed in terms of the following modification of (1) [57]:

$$\hat{F}(t) = \hat{\dot{y}}(t) - \alpha\, u(t). \tag{6}$$

A first-order derivative plus low-pass filter is suggested in [62] in the practical estimation of the derivates of the controlled output $y(t)$ in (1) and the reference trajectory $r(t)$ in (3). The transfer function of that filter is $F(s)$ [57]

$$F(s) = \frac{K_{Lp1} s}{1 + T_{Lp1} s}, \tag{7}$$

where $K_{Lp1}$ is the filter gain and $T_{Lp1}$ is the filter time constant. These two filter parameters should be chosen according to the recommendation formulated in [57] in order to obtain accurate derivative estimates characterized by small estimation errors and derivatives smoothing, as a compromise to noise reduction and the delay it induces. This filter generates both $\dot{r}(t)$ in (4) (the filtered derivative of $r(t)$) and the estimate of $\dot{y}(t)$, with the notation $\hat{\dot{y}}(t)$, which leads to (6) [57].

The MFC structure with iPI controller is presented in Figure 1, and details on the dynamics of the control system structure are given in [57]. The estimation error $e_{est}(t)$ of $F(t)$, whose value is considered negligible in the design, is defined as [57]

$$e_{est}(t) = \dot{y}(t) - \hat{\dot{y}}(t) = F(t) - \hat{F(t)}. \tag{8}$$

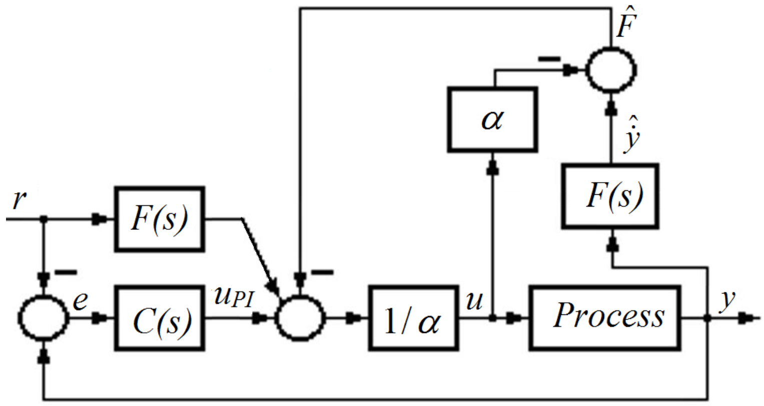


Figure 1: MFC structure with iPI controller [62]

As shown in Figure 1 and (2), the tracking error equals the minus control error. This solution to present the theory was adopted in accordance with the seminal papers on MFC [19], [20] and [21], and also to simplify the control system structures that will be presented as follows in order to avoid the need of many minuses.

The design approach of the iPI controller consists of the following steps:

*Step iPI1.* Set the design parameter $\alpha > 0$ such that the terms $\dot{y}(t)$ and $\alpha\, u(t)$ have the same order of magnitude.

*Step iPI2.* Choose the parameters of the first-order derivative plus low-pass filter with the transfer function $F(s)$ in (7), such that to respect the recommendation given above.

*Step iPI3.* Tune the parameters $K_P$ and $K_I$ of the PI controller component of the iPI controller. These parameters are optimally tuned as solutions to the optimization problems defined in Section 4 and solved in terms of GWO.

The first data-driven model-free sliding mode controller is developed in [56] and [57], and the expression of the control law is [57]

$$u(t) = \frac{1}{\alpha}\left(-\hat{F}(t) + \dot{r}(t) - \frac{e(t)}{T} - e_{est\,\max} - \frac{\eta}{T}\,\mathrm{sat}(\sigma(t), \varepsilon)\right), \tag{9}$$

where $T > 0$ is the design parameter that prescribes the desired behavior of the control system on the sliding mode manifold $\sigma(t) = 0$, with

$$\sigma(t) = \int_0^t e(\tau)d\tau + T\, e(t), \tag{10}$$

$e_{est\ \max}$ is the upper bound of $|e_{est}(t)|$ [57]

$$|e_{est}(t)| \leq e_{est\,\max}, \tag{11}$$

and the nonlinear switching term in (9) specific to the correction control signal that guarantees the fulfillment of the sliding mode reaching and existence condition [57]

$$\sigma(t)\ \dot{\sigma}(t) < 0 \tag{12}$$

is expressed as follows in the framework of the boundary layer approach to mitigate the chattering effects:

$$\frac{\eta}{\alpha\, T}\ \mathrm{sat}(\sigma(t), \varepsilon) = \frac{\eta}{\alpha\, T}\begin{cases} -1 & \text{if } \sigma(t) < -\varepsilon, \\ \frac{\sigma(t)}{\varepsilon} & \text{if } |\sigma(t)| \leq \varepsilon, \\ 1 & \text{if } \sigma(t) > \varepsilon, \end{cases} \tag{13}$$

where $\eta > 0$ is the convergence factor and the $\varepsilon > 0$ is the boundary layer thickness.

The control system structure with first data-driven model-free sliding mode controller is illustrated in Figure 2. The theoretical justification of the design, which makes use of a Lyapunov function candidate, is offered in [56] and [57].

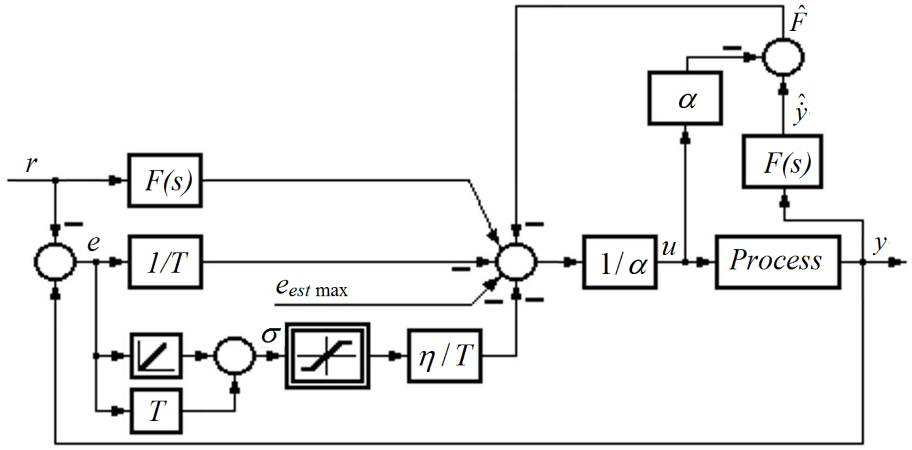


Figure 2: Control system structure with first data-driven model-free sliding mode controller [62]

The design approach of the first data-driven model-free sliding mode controller consists of the following steps as a modification of the approach given in [57], where SM indicates Sliding Mode and the first digit 1 indicates this first controller:

*Step SM1.1.* Set the design parameter $\alpha > 0$ such that the terms $\dot{y}(t)$ and $\alpha\, u(t)$ have the same order of magnitude.

*Step SM1.2.* Choose the parameters of the first-order derivative plus low-pass filter with the transfer function $F(s)$ in (7), such that to respect the recommendation given at the iPI controller.

*Step SM1.3.* Tune the parameters $e_{est\,\max}$, $T$, $\eta$ and $\varepsilon$ of the first data-driven model-free sliding mode controller. These parameters are optimally tuned as solutions to the optimization problems defined in Section 4 and solved in terms of GWO. The parameters $\eta > 0$ and $\varepsilon > 0$ should fulfill the conditions [57]

$$|\sigma(t)|\,\eta > 2\,T\,e_{est\,\max}, \tag{14}$$

$$0 = -\frac{\eta\,\sigma_\infty}{\varepsilon} + T\,[e_{est\,\infty} - e_{est\,\max}], \tag{15}$$

where $e_{est\,\infty}$ is the steady-state estimation error.

The second data-driven model-free sliding mode controller is developed in [57], and the expression of the control law is [57]

$$\begin{aligned} u(t) = \frac{1}{\alpha}\Big[&-\hat{F}(t) + \dot{r}(t) - K_P e(t) - K_I \textstyle\int_0^t e(\tau)d\tau \\ &-\frac{1}{T}\left(\delta\alpha T + \psi + T\,e_{est\,\max} + |K_I T \textstyle\int_0^t e(\tau)d\tau + (K_P T - 1)e(t)|\right) sgn(\sigma(t))\Big], \end{aligned} \tag{16}$$

where $\psi > 0$ and $\delta > 0$ are design parameters inserted in [57] in order to ensure the fulfillment of the sliding mode reaching and existence condition (12). The parameter $\psi$ is a reserve in the fulfillment of this condition, and it is recommended in this regard in [57] that $\delta$ should be large enough to suppress all bounded uncertainties and unstructured system dynamics.

The control system structure with second data-driven model-free sliding mode controller is presented in Figure 3. The theoretical justification of the design is given in [57].

The design approach of the second data-driven model-free sliding mode controller consists of the following steps as a modification of the approach given in [57], where the first digit 2 indicates this second controller:

*Step SM2.1.* Set the design parameter $\alpha > 0$ such that the terms $\dot{y}(t)$ and $\alpha\, u(t)$ have the same order of magnitude.

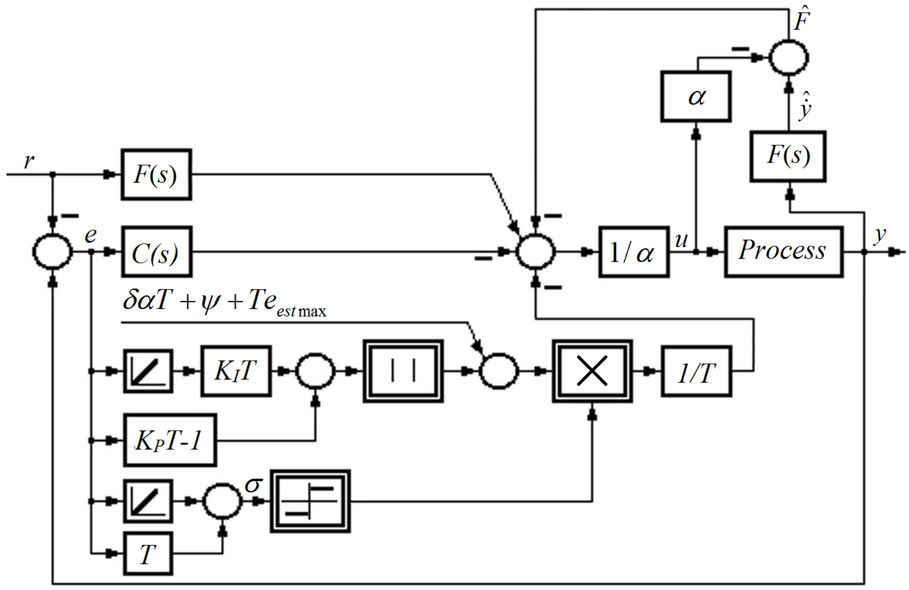


Figure 3: Control system structure with second data-driven model-free sliding mode controller [57]

*Step SM2.2.* Choose the parameters of the first-order derivative plus low-pass filter with the transfer function $F(s)$ in (7), such that to respect the recommendation given at the iPI controller.

*Step SM2.3.* Tune the parameters $K_P$ and $K_I$ of the PI controller component and the parameters $e_{est\max}$, $T$, $\psi$ and $\delta$ of the second data-driven model-free sliding mode controller. These parameters are optimally tuned as solutions to the optimization problems defined in Section 4 and solved in terms of GWO. The parameters $\psi > 0$ and $\delta > 0$ should fulfill the steady-state condition [57]

$$\begin{array}{l} K_IT\ \int_0^t e(\tau)d\tau + (K_PT-1\ )\ e(t) + (\psi + |K_IT\ \int_0^t e(\tau)d\tau + (K_PT-1)e(t)| \\ +T\ e_{est\ \max} + \alpha T\delta)sgn(\sigma(t)) = T\ e_{est\,\infty}. \end{array} \tag{17}$$

## 3 Data-driven model-free fuzzy controller

The data-driven model-free fuzzy controller is built upon the expression (4) of the control law of the iPI controller. Using the notations

$$\begin{array}{l} z_1(t) = \int_0^t e(\tau)d\tau, \\ z_2(t) = e(t), \end{array} \tag{18}$$

for the input and also scheduling variables $z_1(t)$ and $z_2(t)$ of the continuous-time data-driven model-free fuzzy controller in Takagi-Sugeno form, the expression of the output $u_{PI}(t)$ of the PI controller component in (4) becomes

$$u_{PI}(t) = K_P z_2(t) + K_I z_1(t). \tag{19}$$

The output $u_{PI}(t)$ of the PI controller component given in (19) is replaced by the output $u_{TISO-FC}(t)$ of the data-driven model-free fuzzy controller, where TISO-FC indicates a Two Inputs-Single Output Fuzzy Controller. The control system structure with data-driven model-free fuzzy controller is illustrated in Figure 4. The input membership functions are also given in Figure 4.

The fuzzy component of the data-driven model-free fuzzy controller is designed around the nonlinear TISO-FC (the strictly speaking fuzzy controller), with the parameters $B_{z1} > 0$ and $B_{z2} > 0$ of the input membership functions. The inference engine of TISO-FC uses the SUM and PROD operators, and the rule base is presented in Table 1, with the rule consequents

$$\begin{array}{l} u_{PI}(t) = K_P z_2(t) + K_I z_1(t), \\ \Phi_i(t) = \sigma_i u_{PI}(t),\ i = 1 \ldots 3, \end{array} \tag{20}$$

which point out the three tuning parameters $\sigma_1$, $\sigma_2$ and $\sigma_3$. More linear controllers can be used in the rule consequents, however the purpose is to get cost-effective fuzzy controllers. Table 1 shows that the

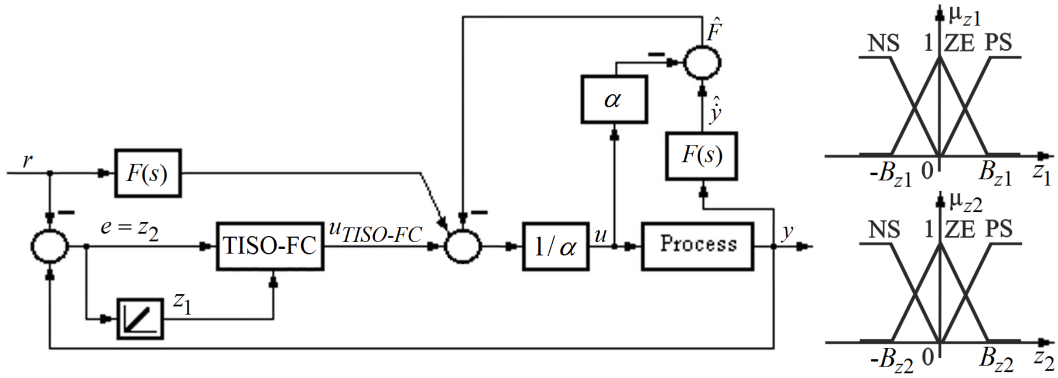


Figure 4: Control system structure with data-driven model-free fuzzy controller and input (scheduling) membership functions

rule base consists of only three rules, which make the fuzzy component of the controller behave, as specified in Section 1, as a bump-less interpolator between three separately designed continuous-time PI controllers placed in the rule consequents. The weighted sum method is used in the defuzzification module of TISO-FC.

Table 1
Rule base of TISO-FC

| $z_1(t)$ $z_2(t)$ | NS | ZE | PS |
|---|---|---|---|
| PS | $\Phi_2(t)$ | $\Phi_2(t)$ | $\Phi_3(t)$ |
| ZE | $\Phi_1(t)$ | $\Phi_2(t)$ | $\Phi_1(t)$ |
| NS | $\Phi_3(t)$ | $\Phi_2(t)$ | $\Phi_2(t)$ |

The modal equivalence principle is usually used to make the fuzzy component close to a linear PI controller. However, this principle is not applied to this controller in order to benefit by the additional degree of freedom brought by the nonlinearity that replaces the linear PI controller component in (4).

The design approach of the data-driven model-free fuzzy controller consists of the following steps, where FC indicates the fuzzy controller:

*Step FC1.* Set the design parameter $\alpha > 0$ such that the terms $\dot{y}(t)$ and $\alpha\, u(t)$ have the same order of magnitude.

*Step FC2.* Choose the parameters of the first-order derivative plus low-pass filter with the transfer function $F(s)$ in (7), such that to respect the recommendation given in the previous section.

*Step FC3.* Tune the parameters $K_P$ and $K_I$ of the linear part and the parameters $B_{z1}$, $B_{z2}$, $\sigma_1$, $\sigma_2$ and $\sigma_3$ of the nonlinear part of the data-driven model-free fuzzy controller. These parameters are optimally tuned as solutions to the optimization problems defined in the next section and solved in terms of GWO.

# 4 Validation and experimental results

## 4.1 The 3D crane system

The following nonlinear state-space equations of the process are obtained if no disturbances are considered accepting zero initial conditions for all state variables except $x_1$ [31], [49]:

$$\begin{aligned}
&\dot{x}_1 = x_2,\\
&\dot{x}_2 = -T_1x_2 - T_{sy}sgn(x_2) - \mu_1\cos(x_5)[-T_3x_{10} - T_{sz}sgn(x_{10})] + k_1u_1 + k_3\mu_1\cos(x_5)u_3,\\
&\dot{x}_3 = x_4,\\
&\dot{x}_4 = -T_2x_4 - T_{sx}sgn(x_4) - \mu_2\sin(x_5)\sin(x_7)[-T_3x_{10} - T_{sz}sgn(x_{10})] + k_2u_2 + k_3\mu_2\sin(x_5)\sin(x_7)u_3,\\
&\dot{x}_5 = x_6,\\
&\dot{x}_6 = -[T_1x_2 - T_{sy}sgn(x_2)]\sin(x_5)/x_9 + \sin(x_3)\cos(x_5)x_8^2/x_9 + \cos(x_5)\cos(x_7)[k_1\sin(x_5)u_1\\
&-k_2\cos(x_5)\sin(x_7)u_2 - k_3\mu_2\sin(x_5)\cdot\cos(x_5)\sin^2(x_7)u_3 + k_3\mu_1\sin(x_5)\cos(x_5)u_3]/x_9^2 + \mu_2\sin(x_5)\cos(x_5)\\
&\cdot\sin^2(x_7)[-T_3x_{10} - T_{sz}sgn(x_{10})]/x_9 + \cos(x_5)\sin(x_7)[T_2x_4 + T_{sx}sgn(x_4)]/x_9 - \mu_1\sin(x_5)\cos(x_5)[-T_3x_{10}\\
&-T_{sz}sgn(x_{10})]/x_9 - 2x_6x_{10}/x_9,\\
&\dot{x}_7 = x_8,\\
&\dot{x}_8 = k_2\sin(x_7)\cos(x_7)u_2/[x_9^2\sin^2(x_5)] - k_3\mu_1\mu_2\sin^2(x_7)\cos(x_7)\cdot u_3/[x_9^2\sin(x_5)]\\
&+\mu_2\sin(x_7)\cos(x_7)[-T_3x_{10} - T_{sz}sgn(x_{10})]/x_9 - 2x_8x_{10}/x_9 + \cos(x_7)[T_2x_4 + T_{sx}sgn(x_4)]/[x_9\sin(x_5)],\\
&\dot{x}_9 = x_{10},\\
&\dot{x}_{10} = \cos(x_5)[T_1x_2 + T_{sy}sgn(x_2)] + x_8^2x_9\sin^2(x_5) - k_1\sin(x_5)\cos(x_5)\cdot\cos(x_7)u_1\\
&-k_2\sin^2(x_5)\sin(x_7)\cos(x_7)u_2 + k_3\sin(x_5)\cos(x_7)[-\mu_2\cdot\sin^2(x_5)\sin^2(x_7) - \mu_1\cos^2(x_5) - 1]u_3\\
&+\mu_2\sin^2(x_5)\sin^2(x_7)[-T_3x_{10} - T_{sz}sgn(x_{10})] + \sin(x_5)\sin(x_7)[T_2x_4 + T_{sx}sgn(x_4)] + \mu_1[-T_3x_{10} - T_{sz}\\
&\cdot sgn(x_{10})] + \mu_1\sin^2(x_5)[-T_3x_{10} - T_{sz}sgn(x_{10})] + x_6^2x_9 - T_3x_{10} - T_{sz}sgn(x_{10}),
\end{aligned} \tag{21}$$

where the state variables are $x_1$ – the distance of the cart from the center of the rail, $x_{10}$ – the initial condition for $x_1$, $x_2$ – the speed of the cart on the direction of $x_1$, $x_3$ – the distance of the rail with the cart from the center of the construction frame, $x_4$ – the speed of the rail with the cart on the direction of $x_3$, $x_5$ – the acute angle between the lift-line of the payload and the rail, $x_6$ – the angular speed that corresponds to $x_5$, $x_7$ – the acute angle between the lift-line of the payload and the vertical line, $x_8$ – the angular speed that corresponds to $x_7$, $x_9$ – the length of the lift-line and also the payload position controlled in this paper, and $x_{10}$ – the speed of the lift-line. The control signals $u_1$, $u_2$ and $u_3$ correspond to the Pulse Width Modulation (PWM) duty cycles applied to the Direct Current (DC) motors that actuate the system on the axes $x_1$, $x_3$ and $x_9$. Axis $x_1$ is referred to as x-axis, $x_3$ is referred to as y-axis, and $x_9$ is referred to as z-axis. The parameters of the 3D crane system are obtained using the first principles models of the process [31], [49]

$$\begin{aligned}
&\mu_1 = 0.4156,\ \mu_2 = 0.1431,\ k_1 = 49.8636, k_2 = 16.0336,\ k_3 = -129.8258,\\
&T_1 = 11.5242 \text{ s},\ T_2 = 26.3263 \text{ s},\ T_3 = 217.3535 \text{ s},\ T_{sx} = 1.4903 \text{ s},\ T_{sy} = 6.4935 \text{ s},\ T_{sz} = 20.8333 \text{ s}.
\end{aligned} \tag{22}$$

The state variables $x_1$, $x_3$, $x_5$, $x_7$ and $x_9$ represent the controlled outputs of the 3D crane. The choice of these state variables depends on the specific control problems, where state variables $x_1$, $x_3$ are the controlled outputs of the crane position control problems, and state variables $x_5$, $x_7$ and $x_9$ are the controlled outputs used in anti-swing control problems.

The simplified model of the 3D crane system is obtained in terms of considering that only the forces on the three axes $x_1$, $x_3$ and $x_9$ affect the movement of the system. Thus, the following transfer functions, $H_x(s)$, $H_y(s)$ and $H_z(s)$, which represent the linear version of the 3D crane system simplified model are obtained considering zero initial conditions [31], [49]:

$$\begin{aligned}
H_x(s) &= x_1(s)/u_1(s) = k_x/[s(1 + T_xs)],\\
H_y(s) &= x_3(s)/u_2(s) = k_y/[s(1 + T_ys)],\\
H_z(s) &= x_9(s)/u_3(s) = k_z/[s(1 + T_zs)],
\end{aligned} \tag{23}$$

where $k_x$, $k_y$ and $k_z$ are the process gains, and $T_x$, $T_y$ and $T_z$ are the process time constants. The least-squares identification based on real-world input-output data measured from the laboratory equipment leads to the parameter values [70], [71]

$$k_x = 0.2939,\ T_x = 0.0587 \text{ s},\ k_y = 0.2747,\ T_y = 0.0379 \text{ s},\ k_z = 0.1019,\ T_z = 0.0408 \text{ s}. \tag{24}$$

but other parameter values can also be used.

The experimental stand of the 3D crane system laboratory equipment in the Intelligent Control Systems Laboratory of the Politehnica University of Timisoara, Romania, is illustrated in Figure 5.


Figure 5: The experimental stand of 3D crane system laboratory equipment

### 4.2 Experimental setup

The control system structures with iPI controller referred as MFC-iPI, with first data-driven model-free sliding mode controller referred as MFSMC1, with second data-driven model-free sliding mode controller referred as MFSMC2 and with data-driven model-free fuzzy controller referred as MFFC are validated using experiments conducted on the experimental stand to control the payload position $y_3 = x_9$ (Figure 5).

All experiments started in zero initial conditions and no disturbances were applied. The signal

$$-0.18 \;\; if \; t \in (0 \ldots 15), \; 0.18 \;\; if \; t \in (15 \ldots 30), \; -0.09 \;\; if \; t \in (30 \ldots 45), \; 0 \;\; if \; t \in (45 \ldots 60) \tag{25}$$

was applied to the reference model (RM) with the transfer function

$$H_{RM}(s) = \frac{K_{RM}}{1 + T_{RM}s} \tag{26}$$

to produce the reference trajectory $r(t)$ of the payload position $y_3 = x_9$. The two parameters in (26) are $K_{RM}$ – the proportional gain, $K_{RM} = 1$, and $T_{RM}$ – the time constant, $T_{RM} = 0.3$ s, and the duration of an experiment was 60 s.

The optimization problem whose solution is the optimal parameter vector $\rho^{(\diamondsuit)*}$ of the MFC-iPI, MFSMC1, MFSMC2 and MFFC controllers is

$$\boldsymbol{\rho}^{(\diamondsuit)*} = \arg \min_{\boldsymbol{\rho}} J_{e,u}(\boldsymbol{\rho}^{(\diamondsuit)}), \;\; J_{e,u}(\boldsymbol{\rho}^{(\diamondsuit)}) = \int_{t_0}^{t_f} e^2(t, \boldsymbol{\rho}^{(\diamondsuit)}) dt, \tag{27}$$

where $\boldsymbol{\rho}^{(\diamondsuit)}$ is the parameter vector of the MFC-iPI, MFSMC1, MFSMC2 or MFFC controller, $J_{e,u}(\boldsymbol{\rho}^{(\diamondsuit)})$ is the objective function and also performance index that will monitor the performance of control systems with MFC-iPI, MFSMC1, MFSMC2 and MFFC controllers, and the superscript $\diamondsuit$ indicates the controller type whose parameters are optimally determined using GWO as follows: 1 corresponds to the MFC-iPI controller with the expression of the parameter vector $\rho^{(1)}$

$$\boldsymbol{\rho}^{(1)} = [K_P \;\; K_I]^T, \tag{28}$$

2 corresponds to the MFSMC1 controller with the expression of $\boldsymbol{\rho}^{(2)}$

$$\boldsymbol{\rho}^{(2)} = [\varepsilon \;\; T \;\; e_{est \; \max} \;\; \eta]^T, \tag{29}$$

3 corresponds to the MFSMC2 controller with the expression of $\boldsymbol{\rho}^{(3)}$

$$\boldsymbol{\rho}^{(3)} = [K_P \;\; K_I \;\; \psi \;\; T \;\; e_{est \; \max} \;\; \delta]^T, \tag{30}$$

and 4 corresponds to the MFFC controller with the expression of $\boldsymbol{\rho}^{(4)}$:

$$\boldsymbol{\rho}^{(4)} = [K_P \ \ K_I \ \ B_{z1} \ \ B_{z2} \ \ \sigma_1 \ \ \sigma_2 \ \ \sigma_3]^T. \tag{31}$$

All details on the dynamic regimes where the optimization problem defined in (27) is solved are given above. The time horizon related to (27) is $[t_0, t_f] = [0, 60]$ s. An additional detail on the dynamic regime concerns the controlled output in this paper $y_3 = x_9$, where the index 3 points out that this is achieved (as also shown in the transfer function $H_z(s)$ in (23) of the corresponding process sub-system) using the control signal $u_3$. The other two control signals are set to zero, $u_1 = u_2 = 0 \ \forall t \in [t_0, t_f] = [0, 60]$ s.

### 4.3 Experimental results

The parameters of the MFC-iPI, MFSMC1, MFSMC2 and MFFC controllers are obtained in terms of the design steps given in Sections 2 and 3. The last design step is carried out in a model-based manner using the mathematical model of the process expressed in terms of the state-space equations in (21) along with the output equation $y_3 = x_9$, and the dynamic regimes described in the previous sub-section, in order to evaluate the objective function needed in GWO.

The design processes for all controllers in this paper started with executing the steps *iPI1*, *SM1.1*, *SM2.1* and *FC1* in terms of setting parameter $\alpha = 10$ and next the steps *iPI2*, *SM1.2*, *SM2.2* and *FC2*, where the parameters $K_{Lp1} = 0.85$ and $T_{Lp1} = 0.15$ s were set.

The parameters of GWO were set as in [64], namely 20 agents (grey wolves) in the population, and maximum 100 iterations. The dimension of the solution space depends on one of the four data-driven model-free controllers that are actually tuned, and additional details are given in [51]. The optimal parameters of the MFC-iPI controller are obtained going through *step iPI3*:

$$\boldsymbol{\rho}^{(1)} = [70.0124 \ \ -5.7823]^T. \tag{32}$$

The optimal parameters of the MFSMC1 controller are obtained going through *step SM1.3*,

$$\boldsymbol{\rho}^{(2)} = [0.7988 \ \ 94.0366 \ \ 0.1313 \ \ 99.9678]^T. \tag{33}$$

The optimal parameters of the MFSMC2 controller going through *step SM2.3*,

$$\boldsymbol{\rho}^{(3)} = [70.0124 \ \ -5.7863 \ \ 41.3144 \ \ 86.2046 \ \ 0.6343 \ \ 1.7460]^T. \tag{34}$$

The optimal parameters of the MFFC controller going through *step FC3*,

$$\boldsymbol{\rho}^{(4)} = [70.0124 \ \ -5.7823 \ \ 0.13 \ \ 0.3935 \ \ 1.1 \ \ 4.3 \ \ 0.8]^T. \tag{35}$$

The experimental results of the control system with MFC-iPI, MFSMC1, MFSMC2 and MFFC controllers are synthesized in Figure 6, where the reference input is $y_3^* = r$, and the controlled output is $y_3 = x_9$. The evolution of the control signal is not presented, which is $u_3$ in this paper, where payload position control is exemplified.

The values of the performance index that monitors the performance of the control systems with MFC-iPI, MFSMC1, MFSMC2 and MFFC controllers are presented in Table 2.

Table 2
The objective function

| | MFC-iPI | MFSMC1 | MFSMC2 | MFFC |
|---|---|---|---|---|
| $J_{e,u}(\boldsymbol{\rho}^{(\diamondsuit)})$ | 0.0800 | 0.0979 | 0.0962 | 0.0797 |

The objective function values in Table 2 show an overall small improvement obtained by adding the fuzzy component in the data-driven model-free controller although the steady-state errors after the first two set-point modifications are not favorable as illustrated in Figure 6. The results will be different if other representative applications will be treated, e.g. the control of the other two positions specific to this process but also [4], [11], [74], [58], [2], [13], [6], or other optimization algorithms are involved as, for example, interactive evolutionary optimization [44], population extremal optimization [40], [87], [10], bat algorithm [48], the introduction of information feedback models in metaheuristic algorithms [78], [26], [88], island-based cuckoo search [1] and hybrid swarm algorithms [86].

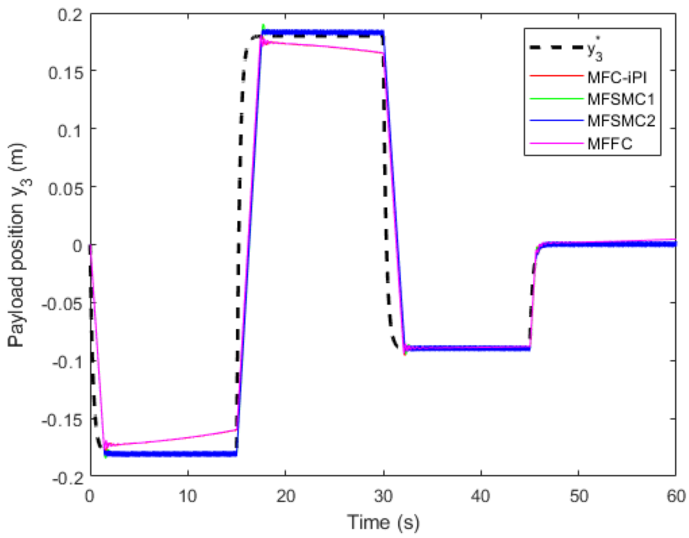


Figure 6: The experimental results of the CS with MFC-iPI, MFSMC1, MFSMC2 and MFFC controllers expressed as reference trajectory and controlled outputs (payload position) versus time

# 5 Conclusions

This paper proposed four data-driven model-free continuous-time control algorithms built around an intelligent Proportional-Integral controller by adding nonlinear components as sliding mode and fuzzy control ones. The results are validated using experiments to control the payload position of 3D crane systems.

The results expressed in a synthesized way in Figure 6 reveal that all four control systems successfully manage to control the payload position of the 3D crane system. The objective function comparison in Table 2 reveals that all MFC-iPI, MFSMC1, MFSMC2 and MFFC controllers perform in the same manner, but the MFFC controller has a small advantage in front of MFC-iPI, MFSMC1, MFSMC2 controllers.

The main limitation of inserting sliding mode and fuzzy control components in the data-driven model-free controller is that the controller structure is complicated but the performance is not improved significantly. Therefore, future research will be focused on the further modification of both sliding mode and fuzzy control components in order to make them more flexible such that to capture the process nonlinearities; the flexibility can be achieved by modifying the fuzzy component structure in both membership functions and rule consequents and considering data-driven model-free sliding mode fuzzy control.

## Funding

This work was supported in part by the grants from the UEFISCDI of the Ministry of Research and Innovation, Romania, project numbers PN-III-P1-1.1-PD-2019-0637, PN-III-P1-1.1-TE-2019-1117, PN-III-P2-2.1-PTE-2019-0694, within PNCDI III, and by the NSERC of Canada.

## Author contributions

The authors contributed equally to this work.

## Conflict of interest

The authors declare no conflict of interest.

## References


[1] Abed-alguni, B.H. (2019). Island-based cuckoo search with highly disruptive polynomial mutation, *International Journal of Artificial Intelligence*, 17(1), 57–82, 2019.

[2] Andoga, R.; Fozo, L. (2017). Near magnetic field of a small turbojet engine, *Acta Physica Polonica A*, 131(4), 1117–1119, 2017.

[3] Angelov, P.; Škrjanc, I.; Blažič, S. (2013). Robust evolving cloud-based controller for a hydraulic plant, *Proceedings of 2013 IEEE Conference on Evolving and Adaptive Intelligent Systems*, Singapore, 1–8, 2013.

[4] Baranyi, P.; Korondi, P.; Patton, R.J.; Hashimoto, H. (2004). Trade-off between approximation accuracy and complexity for TS fuzzy models, *Asian Journal of Control*, 6(1), 21–33, 2004.

[5] Bashir, A.O.; Rui, X.-T.; Zhang, J.-S. (2019). Ride comfort improvement of a semi-active vehicle suspension based on hybrid fuzzy and fuzzy-PID controller, *Studies in Informatics and Control*, 28(4), 421–430, 2019.

[6] Bejinariu, S.-I.; Saramandu, N.; Nevaci, M.; Apopei, V.; Teodorescu, H.-N. (2020). Recovery of old dialectal materials and maps through image processing, *Romanian Journal of Information Science and Technology*, 23(3), 223–237, 2020.

[7] Bouteraa, Y.; Abdallah, I.B.; Elmogy, A.; Ibrahim, A.; Tariq, U.; Ahmad, T. (2020). A fuzzy logic architecture for rehabilitation robotic systems, *International Journal of Computers Communications & Control*, 15(4), 3814, 2020.

[8] Campi, M.C.; Lecchini, A.; Savaresi, S.M. (2002). Virtual reference feedback tuning: a direct method for the design of feedback controllers, *Automatica*, 38(8), 1337–1346, 2002.

[9] Cao, L.; Gao, S.-L.; Zhao, D.-Y. (2020). Data-driven model-free sliding mode learning control for a class of discrete-time nonlinear systems, *Transactions of the Institute of Measurement and Control*, DOI: 10.1177/0142331220921022, 2020.

[10] Chen, M.-R.; Zeng, G.-Q.; Lu, K.-D. (2019). A many-objective population extremal optimization algorithm with an adaptive hybrid mutation operation, *Information Sciences*, 498, 62–90, 2019.

[11] Costin, H.; Rotariu, C.; Alexa, I.; Constantinescu, G.; Cehan, V.; Dionisie, B.; Andruseac, G.; Felea, V.; Crauciuc, E.; Scutariu, M. (2009). TELEMON - A complex system for real time medical telemonitoring, *Proceedings of $11^{th}$ International Congress of the IUPESM/World Congress on Medical Physics and Biomedical Engineering*, Munich, Germany, 92–95, 2009.

[12] da Silva Moreira, J.; Acioli Júnior, G.; Rezende Barros, G. (2018). Time and frequency domain data-driven PID iterative tuning, *IFAC-PapersOnLine*, 51(15), 1056–1061, 2018.

[13] Deliparaschos, K.M.; Michail, K.; Zolotas, A.C. (2020). Facilitating autonomous systems with AI-based fault tolerance and computational resource economy, *Electronics*, 9(5), 788, 2020.

[14] Dombi, J.; Hussain, A. (2019). Data-driven arithmetic fuzzy control using the distending function, in *Ahram, T.; Taiar, R.; Colson, S.; Choplin, A. (eds.), IHIET: Human Interaction and Emerging Technologies*, Springer, Cham, Advances in Intelligent Systems and Computing, 1018, 215–221, 2019.

[15] Dzitac, I.; Filip, F.-G.; Manolescu, M.-J. (2017). Fuzzy logic is not fuzzy: World-renowned computer scientist Lotfi A. Zadeh, *International Journal of Computers Communications & Control*, 12(6), 748–789, 2017.

[16] Ebrahimi, N.; Ozgoli, S.; Ramezani, A. (2018). Model-free sliding mode control, theory and application, *Proceedings of the Institution of Mechanical Engineers Part I Journal of Systems and Control Engineering*, 232(10), 095965181878059, 2018.

[17] Ebrahimi, N.; Ozgoli, S.; Ramezani, A. (2020). Model free sliding mode controller for blood glucose control: Towards artificial pancreas without need to mathematical model of the system, *Computer Methods and Programs in Biomedicine*, DOI: 10.1016/j.cmpb.2020.105663, 2020.

[18] Fan, Q.-Y.; Yang, G.-H. (2016). Adaptive actor-critic design-based integral sliding-mode control for partially unknown nonlinear systems with input disturbances, *IEEE Transactions on Neural Networks and Learning Systems*, 27(1), 165–177, 2016.

[19] Fliess, M.; Join, C. (2009). Model-free control and intelligent PID controllers: Towards a possible trivialization of nonlinear control?, *IFAC Proceedings Volumes*, 42(10), 1531–1550, 2009.

[20] Fliess, M.; Join, C. (2013). Model-free control, *International Journal of Control*, 86(12), 2228–2252, 2013.

[21] Fliess, M.; Join, C.; Mboup, M.; Sira-Ramirez, H. (2006). Vers une commande multivariable sans modele, *Proceedings of Conférence Internationale Francophone d'Automatique*, Bordeaux, France, 1–7, 2006.

[22] Formentin, S.; Campi, M.C.; Caré, A.; Savaresi, S.M. (2019). Deterministic continuous-time Virtual Reference Feedback Tuning (VRFT) with application to PID design, *Systems and Control Letters*, 127, 25–34, 2019.

[23] Gajate, A.; Haber, R.E.; Vega, P.I.; Alique, J.R. (2010). A transductive neuro-fuzzy controller: Application to a drilling process, *IEEE Transactions on Neural Networks*, 21(7), 1158–1167, 2010.

[24] Galluppi, O.; Formentin, S.; Novara, C.; Savaresi, S.M. (2019). Multivariable D2-IBC and application to vehicle stability control, *ASME Journal of Dynamic Systems, Measurement and Control*, 141(10), 1–12, 2019.

[25] Gao, Z. (2006). Active disturbance rejection control: a paradigm shift in feedback control system design, *Proceedings of 2006 American Control Conference*, Minneapolis, MN, USA, 2399–2405, 2006.

[26] Gu, Z.-M.; Wang, G.-G. (2020). Improving NSGA-III algorithms with information feedback models for large-scale many-objective optimization, *Future Generation Computer Systems*, 107, 49–69, 2020.

[27] Guerra, T.M.; Sala, A.; Tanaka, K. (2015). Fuzzy control turns 50: 10 years later, *Fuzzy Sets and Systems*, 281, 168–182, 2015.

[28] Hjalmarsson, H. (2002). Iterative feedback tuning - an overview, *International Journal of Adaptive Control and Signal Processing*, 16(5), 373−395, 2002.

[29] Hou, Z.-S.; Wang, Z. (2013). From Model-based control to data-driven control: Survey, classification and perspective, *Information Sciences*, 235, 3–35, 2013.

[30] Huang, J.-W.; Gao, J.-W. (2020). How could data integrate with control? A review on data-based control strategy, *International Journal of Dynamics and Control*, DOI: 10.1007/s40435-020-00688-x, 2020.

[31] Inteco Ltd. (2008). *3D Crane, User's Manual*, Inteco Ltd., Krakow, Poland, 2008.

[32] Jiang, P.; Cheng, Y.-Q.; Wang, X.-N.; Feng, Z. (2016). Unfalsified visual servoing for simultaneous object recognition and pose tracking, *IEEE Transactions on Cybernetics*, 46(12), 3032–3046, 2016.

[33] Johanyák, Z.C. (2015). A simple fuzzy logic based power control for a series hybrid electric vehicle, *Proceedings of $9^{th}$ IEEE European Modelling Symposium on Mathematical Modelling and Computer Simulation*, Madrid, Spain, 207–212, 2015.

[34] Juang, C.-F.; Chang, Y.-C. (2016). Data-driven interpretable fuzzy controller design through multi-objective genetic algorithm, *Proceedings of 2016 IEEE International Conference on Systems, Man, and Cybernetics*, Budapest, Hungary, 2403–2408, 2016.

[35] Jung, H.; Jeon, K.; Kang, J.-G.; Oh, S. (2021). Iterative feedback tuning of cascade control of two-inertia system, *IEEE Control Systems Letters*, 5(3), 785−790, 2021.

[36] Kadali, R.; Huang, B.; Rossiter, A. (2003). A data driven subspace approach to predictive controller design, *Control Engineering Practice*, 11(3), 261–278, 2003.

[37] Kamesh, R.; Rani, K.Y. (2016). Parameterized data-driven fuzzy model based optimal control of a semi-batch reactor, *ISA Transactions*, 64, 418–430, 2016.

[38] Kammer, L.C.; Bitmead, R.R.; Bartlett, P.L. (2000). Direct iterative tuning via spectral analysis, *Automatica*, 36(9), 1301–1307, 2000.

[39] Karimi, A.; Miskovic, L.; Bonvin, D. (2004). Iterative correlation-based controller tuning, *International Journal of Adaptive Control and Signal Processing*, 18(8), 645–664, 2004.

[40] Li, L.-M.; Lu, K.-D.; Zeng, G.-Q.; Wu, L.; Chen, M.-R. (2016). A novel real-coded population-based extremal optimization algorithm with polynomial mutation: A non-parametric statistical study on continuous optimization problems, *Neurocomputing*, 174, 577–587, 2016.

[41] Li, S.; Ahn, C.K.; Xiang, Z.-R. (2019). Adaptive fuzzy control of switched nonlinear time-varying delay systems with prescribed performance and unmodeled dynamics, *Fuzzy Sets and Systems*, 371, 40–60, 2019.

[42] Lucchini, A.; Formentin, S.; Corno, M.; Piga, D.; Savaresi, S.M. (2020). Torque vectoring for high-performance electric vehicles: a data-driven MPC approach, *IEEE Control Systems Letters*, 4(3), 725–730, 2020.

[43] McDaid, A.J.; Aw, K.C.; Haemmerle, E.; Xie, S.Q. (2012). Control of IPMC actuators for microfluidics with adaptive "online" iterative feedback tuning, *IEEE/ASME Transactions on Mechatronics*, 17(4), 789–797, 2012.

[44] Mls, K.; Cimler, R.; Vaščák, J.; Puheim, M. (2017). Interactive evolutionary optimization of fuzzy cognitive maps, *Neurocomputing*, 232, 58–68, 2017.

[45] Nguyen, A.-T.; Taniguchi, T.; Eciolaza, L.; Campos, V.; Palhares, R.; Sugeno, M. (2019). Fuzzy control systems: past, present and future, *IEEE Computational Intelligence Magazine*, 14(1), 56–68, 2019.

[46] Novara, C.; Formentin, S.; Savaresi, S.M.; Milanese, M. (2015). A data-driven approach to nonlinear braking control, *Proceedings of 54$^{th}$ IEEE Conference on Decision and Control*, Osaka, Japan, 1–6, 2015.

[47] Ontiveros-Robles, E.; Melin, P.; Castillo, O. (2018). Comparative analysis of noise robustness of type 2 fuzzy logic controllers, *Kybernetika*, 54(1), 175–201, 2018.

[48] Osaba, E.; Yang, X.S.; Fister Jr, I.; Del Ser, J.; Lopez-Garcia, P.; Vazquez-Pardavila, A.J. (2019). A discrete and improved bat algorithm for solving a medical goods distribution problem with pharmacological waste collection, *Swarm and Evolutionary Computation*, 44, 273–286, 2019.

[49] Precup R.-E.; Enache, F.-C.; Radac, M.-B.; Petriu, E. M.; Preitl, S; Dragos, C.-A. (2013). Lead-lag controller-based iterative learning control algorithms for 3D crane systems, in *Madarász, L.; Živčák J. (eds.), Aspects of Computational Intelligence: Theory and Applications*, Springer, Berlin, Heidelberg, 2, 25–38, 2013.

[50] Precup, R.-E.; Angelov, P.; Costa, B.S.J.; Sayed-Mouchaweh, M. (2015). An overview on fault diagnosis and nature-inspired optimal control of industrial process applications, *Computers in Industry*, 74, 75–94, 2015.

[51] Precup, R.-E.; David, R.-C.; Petriu, E.M.; Szedlak-Stinean, A.-I.; Bojan-Dragos, C.-A. (2016). Grey wolf optimizer-based approach to the tuning of PI-fuzzy controllers with a reduced process parametric sensitivity, *IFAC-PapersOnLine*, 49(5), 55–60, 2016.

[52] Precup, R.-E.; Preitl, S. (2003). Development of fuzzy controllers with non-homogeneous dynamics for integral-type plants, *Electrical Engineering*, 85(3), 155–168, 2003.

[53] Precup, R.-E.; Preitl, S. (2004). Sensitivity analysis of a class of fuzzy controlled mobile robots, *IFAC Proceedings Volumes*, 37(16), 115–120, 2004.

[54] Precup, R.-E.; Preitl, S. (2006). Stability and sensitivity analysis of fuzzy control systems. Mechatronics applications, *Acta Polytechnica Hungarica*, 3(1), 61–76, 2006.

[55] Precup, R.-E.; Preitl, S.; Petriu, E.M.; Roman, R.-C.; Bojan-Dragos, C.-A.; Hedrea, E.-L.; Szedlak-Stinean, A.-I. (2020). A center manifold theory-based approach to the stability analysis of state feedback Takagi-Sugeno-Kang fuzzy control systems, *Facta Universitatis, Series: Mechanical Engineering*, 18(2), 189–204, 2020.

[56] Precup, R.-E.; Radac, M.-B.; Petriu, E.M.; Dragos, C.-A.; Preitl, S. (2014). Model-free tuning solution for sliding mode control of servo systems, *Proceedings of $8^{th}$ Annual IEEE International Systems Conference*, Ottawa, ON, Canada, 30–35, 2014.

[57] Precup, R.-E.; Radac, M.-B.; Roman, R.-C.; Petriu, E.M. (2017). Model-free sliding mode control of nonlinear systems: Algorithms and experiments, *Information Sciences*, 381, 176–192, 2017.

[58] Precup, R.-E.; Tomescu, M.L. (2015). Stable fuzzy logic control of a general class of chaotic systems, *Neural Computing and Applications*, 26(3), 541–550, 2015.

[59] Precup, R.-E.; Voisan, E.-I.; Petriu, E.M.; Tomescu, M.L.; David, R.-C.; Szedlak-Stinean, A.-I.; Roman, R.-C. (2020). Grey wolf optimizer-based approaches to path planning and fuzzy logic-based tracking control for mobile robots, *International Journal of Computers Communications & Control*, 15(3), 3844, 2020.

[60] Preitl, S.; Precup, R.-E.; Preitl, Z. (2005). Sensitivity analysis of low cost fuzzy controlled servo systems, *IFAC Proceedings Volumes*, 38(1), 342–347, 2005.

[61] Preitl, S.; Precup, R.-E.; Preitl, Z.; Vaivoda, S.; Kilyeni, S.; Tar, J.K. (2007). Iterative feedback and learning control. Servo systems applications, *IFAC Proceedings Volumes*, 40(8), 16–27, 2007.

[62] Roman, R.-C.; Precup, R.-E.; Bojan-Dragos, C.-A.; Szedlak-Stinean, A.-I. (2019). Combined model-free adaptive control with fuzzy component by virtual reference feedback tuning for tower crane systems, *Procedia Computer Science*, 162, 267–274, 2019.

[63] Roman, R.-C.; Precup, R.-E.; David, R.-C. (2018). Second order intelligent proportional-integral fuzzy control of twin rotor aerodynamic systems, *Procedia Computer Science*, 139, 372–380, 2018.

[64] Roman, R.-C.; Precup, R.-E.; Petriu, E.M. (2020). Hybrid data-driven fuzzy active disturbance rejection control for tower crane systems, *European Journal of Control*, DOI: 10.1016/j.ejcon.2020.08.001, 2020.

[65] Roman, R.-C.; Precup, R.-E.; Petriu, E.M.; Dragan, F. (2019). Combination of data-driven active disturbance rejection and Takagi-Sugeno fuzzy control with experimental validation on tower crane systems, *Energies*, 12(8), 1–19, 2019.

[66] Roman, R.-C.; Precup, R.-E.; Petriu, E.M.; Hedrea, E.-L.; Bojan-Dragos, C.-A.; Radac, M.-B. (2019). Model-free adaptive control with fuzzy component for tower crane systems, *Proceedings of 2019 IEEE International Conference on Systems, Man and Cybernetics*, Bari, Italy, 1384–1389, 2019.

[67] Roman, R.-C.; Precup, R.-E.; Radac, M.-B. (2017). Model-free fuzzy control of twin rotor aerodynamic systems, *Proceedings of 25$^{th}$ Mediterranean Conference on Control and Automation*, Valletta, Malta, 559–564, 2017.

[68] Safonov, M.G.; Tsao, T.-C. (1997). The unfalsified control concept and learning, *IEEE Transactions on Automatic Control*, 42(6), 843–847, 1997.

[69] Sato, T.; Kusakabe, T.; Himi, K.; Arakim N.; Konishi, Y. (2020). Ripple-free data-driven dual-rate controller using lifting technique: Application to a physical rotation system, *IEEE Transactions on Control Systems Technology*, DOI: 10.1109/TCST.2020.2988613, 2020.

[70] Schulken, E.; Crassidis, A. (2018). Model-free sliding mode control algorithms including application to a real-world quadrotor, *Proceedings of 5$^{th}$ International Conference of Control, Dynamic Systems, and Robotics*, Niagara Falls, Canada, 112-1–112-9, 2018.

[71] Shamloo, N.F.; Kalat, A.A.; Chisci, L. (2020). Indirect adaptive fuzzy control of nonlinear descriptor systems, *European Journal of Control*, 51, 30–38, 2020.

[72] Simani, S.; Alvisi, S.; Venturini, M. (2015). Data-driven design of a fault tolerant fuzzy controller for a simulated hydroelectric system, *IFAC-PapersOnLine*, 48(21), 1090–1095, 2015.

[73] Spall, J.C.; Cristion, J.A. (1998). Model-free control of nonlinear stochastic systems with discrete-time measurements, *IEEE Transactions on Automatic Control*, 43(9), 1198–1210, 1998.

[74] Teodorescu, H.-N. (2012). Characterization of nonlinear dynamic systems for engineering purposes - a partial review, *International Journal of General Systems*, 41(8), 805–825, 2012.

[75] Touhami, M.; Hazzab, A.; Mokhtari, F.; Sicard, P. (2019). Active disturbance rejection controller with ADRC-fuzzy for MAS control, *Electrotehnică, Electronică, Automatică (EEA)*, 67(2), 89–97, 2019.

[76] Van Waarde, H.J.; Eising, J.; Trentelman, H.L.; Camlibel, M.K. (2020). Data informativity: a new perspective on data-driven analysis and control, *IEEE Transactions on Automatic Control*, DOI: 10.1109/TAC.2020.2966717, 2020.

[77] Vrkalovic, S.; Lunca, E.-C.; Borlea, I.-D. (2018). Model-free sliding mode and fuzzy controllers for reverse osmosis desalination plants, *International Journal of Artificial Intelligence*, 16(2), 208–222, 2018.

[78] Wang, G.-G.; Tan, Y. (2019). Improving metaheuristic algorithms with information feedback models, *IEEE Transactions on Cybernetics*, 49(2), 542–555, 2019.

[79] Wang, H.-P.; Ye, X.-F.; Tian, Y.; Christov, N. (2015). Attitude control of a quadrotor using model free based sliding model controller, *Proceedings of 2015 20$^{th}$ International Conference on Control Systems and Science*, Bucharest, Romania, 149–154, 2015.

[80] Wang, X.-F.; Li, X.; Wang, J.-H.; Fang, X.-K.; Zhu, X.-F. (2016). Data-driven model-free adaptive sliding mode control for the multi degree-of-freedom robotic exoskeleton, *Information Sciences*, 327, 246–257, 2016.

[81] Wang, Z.H.; Liu, Z.; Chen, C.L.P.; Zhang, Y. (2019). Fuzzy adaptive compensation control of uncertain stochastic nonlinear systems with actuator failures and input hysteresis, *IEEE Transactions on Cybernetics*, 49(1), 2–13, 2019.

[82] Wu, H.-N.; Wang, J.-W.; Li, H.-X. (2012). Design of distributed H fuzzy controllers with constraint for nonlinear hyperbolic PDE systems, *Automatica*, 48(10), 2535–2543, 2012.

[83] Yang, X.Z.; Lam, H.-K.; Wu, L.G. (2019). Membership-dependent stability conditions for type-1 and interval type-2 T-S fuzzy systems, *Fuzzy Sets and Systems*, 356, 44–62, 2019.

[84] Yu, W.; Wang, R.; Bu, X.-H.; Hou, Z.-S. (2020). Model free adaptive control for a class of nonlinear systems with fading measurements, *Journal of The Franklin Institute*, 357(12), 7743–7760, 2020.

[85] Zamanipour, M. (2020). A novelty in Blahut-Arimoto type algorithms: Optimal control over noisy communication channels, *IEEE Transactions on Vehicular Technology*, 69(6), 6348–6358, 2020.

[86] Zapata, H.; Perozo, N.; Angulo, W.; Contreras, J. (2020). A hybrid swarm algorithm for collective construction of 3D structures, *International Journal of Artificial Intelligence*, 18(1), 1–18, 2020.

[87] Zeng, G.-Q.; Xie, X.-Q.; Chen, M.-R.; Weng, J. (2019). Adaptive population extremal optimization-based PID neural network for multivariable nonlinear control systems, *Swarm and Evolutionary Computation*, 44, 320–334, 2019.

[88] Zhang, Y.; Wang, G.-G.; Li, K.-Q.; Yeh, W.-C., Jian, M.-W.; Dong, J.-Y. (2020). Enhancing MOEA/D with information feedback models for large-scale many-objective optimization, *Information Sciences*, 522, 1–16, 2020.



*Cite this paper as:*

Precup, R.-E.; Roman, R.-C.; Hedrea, E.-L. ; Petriu, E. M.; Bojan-Dragos, C.-A. (2021). Data-Driven Model-Free Sliding Mode and Fuzzy Control with Experimental Validation, *International Journal of Computers Communications & Control*, 16(1), 4076, 2021.
https://doi.org/10.15837/ijccc.2021.1.4076